

# Photodetector with Internal Aiding Field Based-on GaAs/AlGaAs Heterostructures

A. Cola, F. Quaranta  
CNR IMM, via Arnesano 73100  
Lecce, Italy  
E-mail: [adriano.col@ime.le.cnr.it](mailto:adriano.col@ime.le.cnr.it)

B. Nabet  
ECE Dept., Drexel University,  
Philadelphia, PA, 19104, USA  
E-mail: [nabet@cbis.ece.drexel.edu](mailto:nabet@cbis.ece.drexel.edu)

A. Cataldo  
Dip. Ing. Innovazione, via  
Arnesano 73100 Lecce, Italy  
E-mail: [andrea.cataldo@unile.it](mailto:andrea.cataldo@unile.it)

## Abstract

We present a photodetector that employs a doped GaAs/AlGaAs heterojunction for the dual purpose of barrier height enhancement and creating an internal electric field that aids in the transport and collection of photogenerated electrons. Devices with two doping levels are compared that show the direct effect of the aiding field since all other (optical) parameters remain unchanged. Current-voltage, current-temperature, photocurrent spectra, high-speed time response, and on-wafer frequency domain measurements are reported showing that the device can operate in tens of Giga-Hertz range with low dark current and high responsivity. Small signal model based on frequency domain data is also extracted in order to facilitate photoreceiver design.

## 1. Introduction

The properties of the two-dimensional electron gas (2DEG) formed at the interface of a heterojunction have attracted great attention since its first observation [1], from both perspectives of fundamental physical properties and desirable technological effects. Heterojunctions are now routinely employed in optical sources, be it an LED or a Laser, and optical detectors. One application to optical detection is the use of the widegap material of a heterojunction in order to increase the barrier between metal and narrow gap semiconductor [2]. Confluence of the two properties arising from transverse (to heterojunction interface) transport changes due to band gap differences and lateral transport changes due to electron confinement effects is the focus of the present paper. We use both properties in the design of a light detector that takes advantage of the barrier-enhancing heterojunction to reduce the dark current and noise, while, simultaneously increasing efficiency of

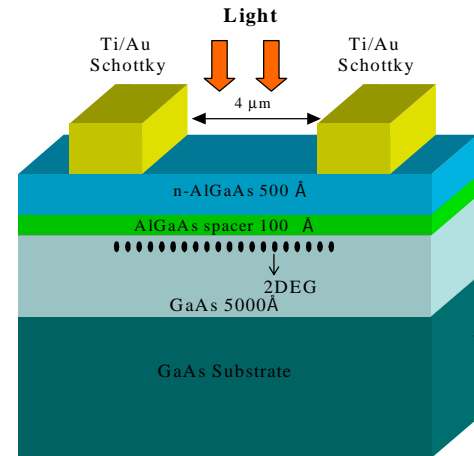


Figure 1: HMSM typical device structure.

collection in the lateral direction due to better transport.

We report here a comprehensive study of these detectors, which also include numerical simulations of the static electrical behavior under bias. We identify the effect of the internal aiding field that results from doping of the widegap material, by comparing two different doping concentrations; thereby ensuring that indeed the electronic properties are responsible for behavior change since the optical properties due to the layered structure remain invariant. Current-Voltage measurements taken as a function of the temperature confirm barrier heights which are higher in the case of the higher AlGaAs doping, with a consistent reduction in the measured dark current.

Concomitant with this effect, which we have previously explained in terms of Coulombic interaction between electron cloud of 2-DEG and electrons emitted

by the metal [3], is the electric field produced in the vertical direction due to modulation doping; we show that this field facilitates transport of optically generated electrons thus improving photoresponsivity. Photoresponse improvement, either under laser excitation and photon energy dependent illumination, is also observed under stationary excitation. High speed time response measurements are given in the last part of this paper that indicate higher peak transient response is achieved in presence of higher 2DEG density without degradation of temporal behavior. The amplitude of the frequency response, as deduced from the FFT, for both cases shows a sharp decline for frequencies greater than 30 GHz. This indicates the suitability of this device for Gigabit Ethernet, 10 Gigabit Ethernet, OC 48 and OC 192 applications. To that end microwave measurements taken in the frequency domain conclude the picture of characterizations, allowing us to extract the elements of the equivalent circuit needed for photoreceiver design.

## 2. Devices design and simulation

The device growth structures is that of an enhancement mode HEMT; on a buffer layer grown on SI-GaAs, 5000 Å of undoped GaAs is deposited followed by 100 Å of undoped spacer layer of  $\text{Al}_{0.24}\text{Ga}_{0.76}\text{As}$  and 500 Å of n-doped  $\text{Al}_{0.24}\text{Ga}_{0.76}\text{As}$ . A low Al mole fraction is chosen so as to ensure a smooth heterointerface and reduce DX centers. The two  $\text{Al}_{0.24}\text{Ga}_{0.76}\text{As}$  doping levels used in this study are  $N_d = 3 \times 10^{17}$  (hereafter called low-doping) and  $6 \times 10^{17} \text{ cm}^{-3}$  (high doping). Two Schottky contacts of 600 Å thickness Ti/Au are deposited on top of the widegap material in an interdigital pattern typically used for photodetectors. The device active area is  $40 \times 40 \mu\text{m}^2$  and a matrix of devices with metal fingers of 1 μm and 2 μm wide and spacing between fingers of 1 μm, 2 μm and 4 μm were used. Figure 1 shows the schematic of the device structure. Since both contacts are rectifying and symmetric, application of voltage reverse-biases one junction and slightly forward biases the other. The reverse biased junction determines current flow while the other mainly controls electron collection. The barrier between metal and AlGaAs thus dominates current flow. This configuration is useful in the study of leakage gate

currents in HEMTs, but has strong application to photodetectors that employ barrier enhancement layers for reduction of dark current [4]. An obvious advantage of this structure is monolithic integrability of the detectors and transistors in both growth and processing that make it suitable for integrated optical detection applications [5].

The structure has been analyzed by the ISE-TCAD<sup>TM</sup> software package in order to simulate the relevant properties. In Fig. 2 the electric field distribution in a low doping device is plotted, clearly showing a strong electric field in the thin AlGaAs layer (peak value of about 300kV/cm). The simulation results confirm that this layer does not contribute to the dark current. Moreover, due to its energy gap value, this layer is transparent to radiation of wavelength greater than 720nm. The GaAs layer is the responsible element for both absorption and current flow. In GaAs under the cathode electrode the peak value of the electric field is about 100kV/cm. The field strongly decreases in the direction along the grounded electrode. In GaAs, the vertical component of the electric field depends on the doping of the AlGaAs layer, in the sense that it increases and it penetrates further into GaAs as the AlGaAs doping increases. This is the aiding field, which pushes the photogenerated electrons toward the AlGaAs/GaAs interface. The electrons drift toward the anode by the applied horizontal field and may be partially transported through the triangular well.

## 3. Static characterization

Current-voltage characteristics under dark have been measured at different temperatures. The curves reported in Fig. 3 refer to the sample with low AlGaAs doping. The sample with high doping shows similar behavior but the activation energy, which is calculated from the slope of the  $\ln(I)$  vs  $1/kT$  plot, is higher. Values at 5V are 0.658eV and 0.677eV for the low- and high-doping samples, respectively. The difference is in agreement with a proposed model [2] based on the repulsion between the electron cloud that is formed in the narrow gap material and the electrons in the metal contact.

The I-V curves for two different doping levels of the AlGaAs, is shown in Fig. 4, in dark and under a 670nm laser illumination.

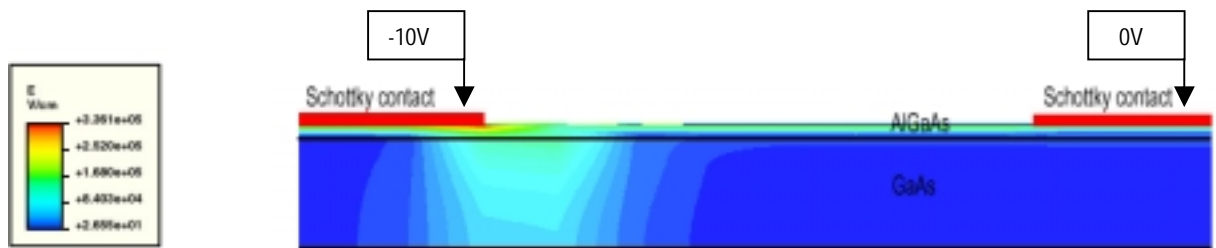


Figure 2: 2D electric field simulated distribution: left contact is 10V biased and the right one 0V.

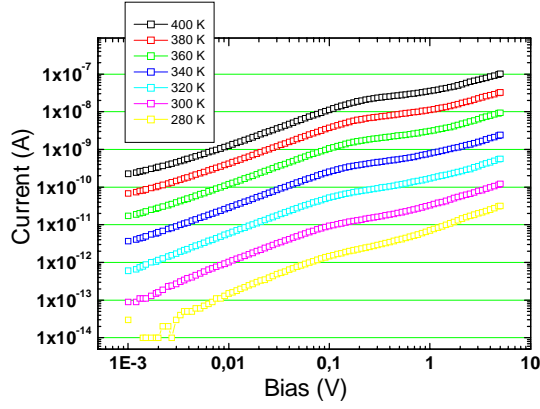


Figure 3: I-V curves under dark at different temperatures for the low doping level device.

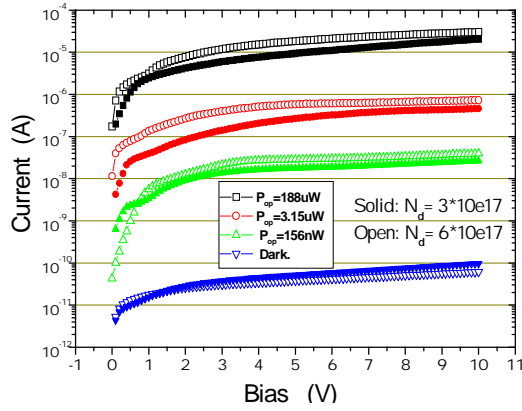


Figure 4: I-V measurements under dark and illumination for two different doping levels.

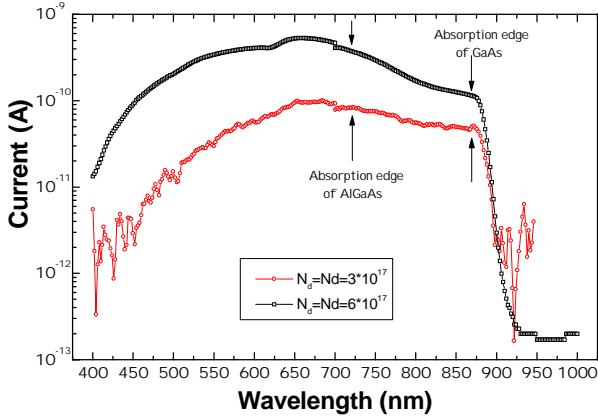


Figure 5: Photocurrent spectra for two different doping levels.

We observe: dark current levels in the tens of picoamps, a large dynamic range due to very low noise levels, that is, more than 5 order of magnitude change is observed for about 0.2mW of optical power, lower dark current and larger photoresponse for higher doping level of AlGaAs.

The spectral response of the low and high-doping samples, in the range of 400-1000 nm, is shown in Fig. 5. It is interesting to note that, in the region where only

GaAs absorbs, as the wavelength decreases, the high-doping sample increases the collection of photo-generated carriers with respect to the low-doping. This result, in conjunction of the data of Fig. 4, is consistent with the aiding role of the vertical electric field, which is stronger in the case of high-doping.

#### 4. Dynamic characterization

The effect of aiding field was also observed in time response to femto-second laser optical pulses. Figure 6 reports a typical trace, which shows a short (less than 10ps long) peak with short full width at half max (FWHM) that is followed by a long (of the order of several hundreds of picoseconds) tail of low amplitude. The inset of the same figure also reports the FFT of the data. Table 1 summarizes the results: for each contact geometry, the peak amplitude and the width of the peak are reported.

Table 1: Comparison of peak amplitude and width of response for different interdigital structures for two doping levels.

Contact Width , Gap (μm)	Amplitude Low-doping (a.u.)	Amplitude high-doping (a.u.)	Width Low-doping (a.u.)	Width high-doping (a.u.)
1,2	0.218	0.239	8.6824E-12	7.739E-12
2,2	0.262	0.364	8.7895E-12	7.744E-12
1,4	0.185	0.216	8.226E-12	7.311E-12
2,4	0.157	0.218	9.259E-12	8.153E-12

The amplitude of the peaks is systematically higher for the high-doping sample and, interestingly, the width of the peak shows a slight decrease thus indicating a faster response. The results show also that the gap affects greatly the peak amplitude, the sample with  $g=2\mu\text{m}$  having higher amplitude than the corresponding with  $g=4\mu\text{m}$ . This is explained in terms reduction of transit time as well as less effective trapping due to decrease in the distance between contacts. By performing the FFT of all the time-traces, we have estimated that the bandwidth of the high doping sample is 2-6 GHz higher than the low doping sample.

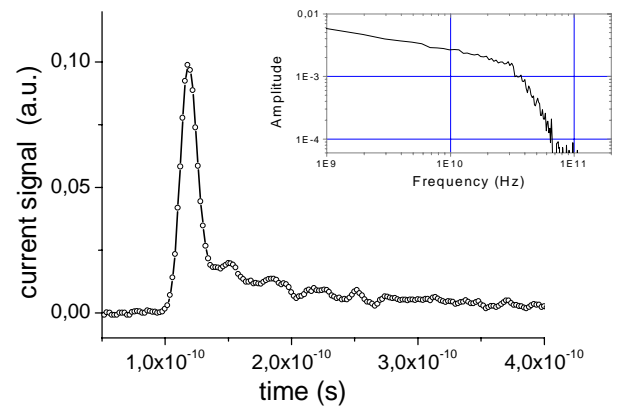


Figure 6: Temporal response of a  $w=2\mu\text{m}$   $g=2\mu\text{m}$  device, inset shows the frequency response.

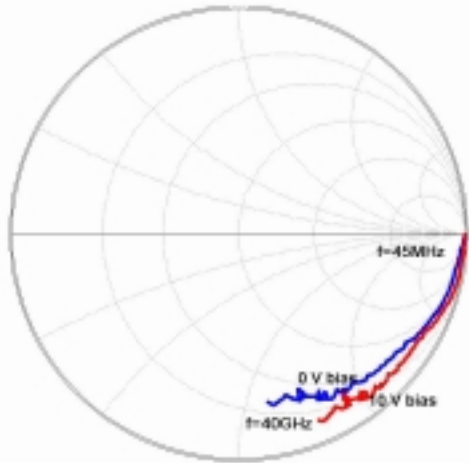


Figure 7: Measured microwave reflection coefficients of a  $w=2\mu\text{m}$   $g=2\mu\text{m}$  device, for 0V and 10V applied DC bias.

Microwave reflection coefficient measurements were performed on-wafer in the frequency range 45 MHz-40GHz by using a network analyzer. The applied bias voltage for each geometrical structure ranged from 0V to 20V. Figure 7 illustrates the typical Smith chart, describing the impedance of a  $w=2\mu\text{m}$   $g=2\mu\text{m}$  device. By using a suitable optimization procedure of the reflection coefficient measured, the equivalent circuit has been identified (for the same device).

Figure 8 shows the equivalent circuit together with the components values that are derived for high voltages ( $V>5\text{V}$ ). These components correspond to:  $C_j$  is junction capacitance,  $R_p$  parallel resistance,  $R_s$  serial resistance,  $C_p$  and  $L_s$  are contacts and leads capacitance and inductance, respectively.

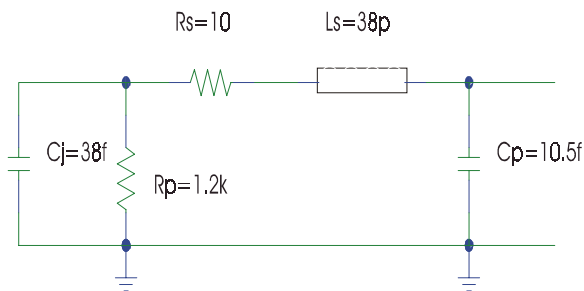


Figure 8: Device equivalent circuit of a  $w=2\mu\text{m}$   $g=2\mu\text{m}$  device.

## 5. Conclusions

We have reported a comprehensive characterization of a photodetector that uses a doped heterojunction to enhance the Schottky barrier and, more importantly, create an internal electric field that aids in the transport and collection of electrons. Devices were compared when the only variant was the doping level thus showing the effect of this internal aiding field. Current-voltage data shows the low dark current and high dynamic range

of the device. Current-temperature data indicate that the activation energy, a measure proportional to the barrier height, increases for the high doping device. This is unexpected if interpreted on the basis of the effect of doping on Schottky barrier lowering, but is consistent with our previous formulation of the repulsion of the thermionically emitted carriers by the electron cloud of the 2DEG. Photocurrent spectra for comparing the two devices show a marked increase at all wavelengths for the high doped device. High speed time response data indicates that the devices easily operate in tens of Gigahertz with the high doped device showing much higher peak of response with no adverse effect, even slight improvement, of rise time and FWHM. Finally on-wafer frequency-domain measurements with a network analyzer were performed which allowed the derivation of an RF small signal model that is necessary for designing complete photoreceivers for optical communication applications. Based on this comprehensive evaluation, we suggest that this heterojunction based device that uses the same technology as the HEMT is an excellent candidate for Gigabit Ethernet, 10 Gigabit Ethernet, OC 48 and OC 192 applications.

## Acknowledgments

The authors thank Prof. U. Pisani, Ing. V. Teppati and Ing. V. Niculae for their support and contribution in the microwave reflection coefficients measurements, and Dr. M. Currie for the cooperation in time response measurements. BN acknowledges the support of the NSF through award ECS 0117073.

## References

- [1] R. Dingle, H. L. Störmer, A.C. Gossard, and W. Wiegmann, "Electron mobilities in modulation-doped semiconductor heterojunction superlattices" *Appl. Phys. Lett.*, 33, (1978), pag. 665.
- [2] J. B. D. Soole and, H. Schumacher, "InGaAs Metal-Semiconductor-Metal Photodetectors for Long-Wavelength Optical Communications" *IEEE, J. of Quantum Electronics*, QE-27, (1992), pag. 737.
- [3] B. Nabet, A. Cola, F. Quaranta, M. Cesareo, R. Rossi, R. Fucci, and A. Anwar, "Electron Cloud effect on current injection across a Schottky contact", *Appl. Phys. Lett.*, 24, (2000), pag.4007.
- [4] C.Y. Chen, Y.M.Pang, K. Alavi, A.Y. Cho and P.A. Garbinski, " Interdigital Al/sub 0.48/In/sub 0.52/ As/Ga/sub 0.47/In/sub 0.53/As photoconductive detectors" *Appl. Phys. Lett.*, 44, (1984), pag. 99.
- [5] M. Horstmann, K. MSM photodetector and 45/85GHz  $f_T/f_{\text{max}}$  HEMT prepared Schimpf, M. Marso, A. Fox, and P. Kordos, "16 GHz bandwidth on an identical InGaAs/InP layer structure" *Electronics Letters*, 32, (1996), pag. 763.